

Short-term variability of proximal femur shape in anteroposterior pelvic radiographs

C. Lindner¹
claudia.lindner@postgrad.manchester.ac.uk
S. Thiagarajah²
J.M. Wilkinson²
arcOGEN Consortium
G.A. Wallis³
T.F. Cootes¹

¹ Imaging Sciences,
The University of Manchester, UK
² Department of Human Metabolism,
University of Sheffield, UK
³ Wellcome Trust Centre for Cell Matrix
Research,
The University of Manchester, UK

Abstract

Anteroposterior (AP) pelvic radiographs only give a 2D projection of what is a 3D shape. Depending on the position of the patient while the radiograph is taken, the 2D projection of the shape may vary. This paper investigates the short-term variability of projected proximal femur shape using AP pelvic radiographs. We train a statistical shape model of the proximal femur based on a set of 87 radiographs—42 of which represent 21 pairs of two radiographs per person taken at two different sessions on the same day. These 21 pairs allow us to use the parameters of the shape model to analyse the within-person variation of projected proximal femur shape. We demonstrate that the within-person variation is small compared to the overall shape variation of the proximal femur given by all 87 radiographs. This work underlines the suitability of AP pelvic radiographs—even though only giving a 2D projection—for the analysis of the relationship between proximal femur shape and diseases such as osteoarthritis or osteoporosis.

1 Introduction

Statistical shape models have been widely used in medical imaging for segmenting structures and capturing their shape variation (see e.g. [1, 2]). Recent research shows evidence that proximal femur shape is related to the susceptibility to medical conditions such as hip osteoarthritis or osteoporotic hip fracture, and that the related risk can be predicted by applying statistical shape models to anteroposterior (AP) pelvic radiographs (see e.g. [3, 4, 5, 6]). However, with AP pelvic radiographs only providing a 2D projection of a 3D shape and the hip joint being a free-moving joint, some of the shape variation may be solely attributable to patient positioning. This study investigates the contribution of within-person shape variation (WPV) to overall shape variation of the proximal femur in AP pelvic radiographs.

2 Methods

2.1 Statistical shape models

Statistical shape models define a deformable model to represent the shape variation of a particular object class, where shape is given by a set of landmarks specifying the boundary of

the object. For a shape model to estimate the shape variation of the object class, it needs to be trained on a set of annotated images. The size of the training set should be large enough such that the shape variation captured is representative for the particular object class. Landmarks should be placed in a consistent way over all training images. Applying a modification of Procrustes analysis to align the shapes of all training images followed by principal component analysis (PCA) allows to describe every shape \mathbf{x}_i of the training set by

$$\mathbf{x}_i = \bar{\mathbf{x}} + \mathbf{P}\mathbf{b}_i \quad (1)$$

where $\bar{\mathbf{x}}$ gives the mean shape over the training set, \mathbf{P} is a matrix of eigenvectors of the covariance matrix over all shapes and represents the modes of the shape model, and \mathbf{b}_i gives the model mode parameters specific to shape \mathbf{x}_i . Once a shape model has been trained, an Active Shape Model (ASM) can be used to find the target object in a new image (see [14]). Given the approximate position of the target object in the new image, the ASM applies an iterative optimisation method to locally move each landmark to a *better* position. The decision making about a better position is based on finding the best match to a local model along the profile normal to the object boundary. For active shape modelling to be successful, the target shape needs to be sufficiently similar to the shapes the model has been trained on, and landmarks should be placed on locally distinctive structures. See [14] for details.

2.2 Data set

This work is based on a set of 87 pelvic radiographs taken in AP view. The image set includes radiographs of 66 individuals. There are 45 single images each of a different person provided by the arcOGEN Consortium and 21 pairs of two radiographs per person provided by J.M. Wilkinson. The latter have been taken under standardised conditions in two separate sessions where the person was asked to walk around between sessions. The single images, however, are not guaranteed to have been taken under standardised conditions. All radiographs were collected under relevant ethical approvals.

2.3 Data annotation

A shape model of the proximal femur was trained based on 87 radiographs. The annotation of the 45 single images was done manually by placing 65 landmarks along the boundary of the proximal femur as shown in Figure 1(a). We chose to use what we call the “front view” of the proximal femur which means that we neither included the greater trochanter nor the lesser trochanter. With AP radiographs giving a 2D projection, depending on the rotation of the leg the lesser trochanter may be “hidden” in some cases as demonstrated in Figure 1(b). Including the lesser trochanter by following the outer boundary of the femoral shaft, hence, would cause the shape model to include variation that is not *true* shape variation but rather is caused by the angle of the 2D projection of a 3D object. A similar reasoning applies to the visibility of parts of the greater trochanter, where the visibility of the lesser and the greater trochanter are correlated due to the vertical rotation axis of the femur.

The annotation of the 21 pairs was done by using an ASM build on the basis of the 45 manually annotated images. Therefore, the 21 pairs were split into four subsets of five or six pairs. Starting with the first subset, one image of each pair has been annotated by an ASM based on the most recent shape model. The shape model was then updated to include the newly annotated images and the resulting ASM was applied to the second of each pair of the first subset. In this manner, each of the four subsets has been gradually annotated and included in the shape model. The reason for splitting the annotation of every pair is to allow

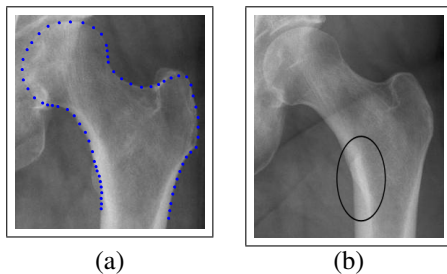


Figure 1: (a) Outline of the proximal femur specified by 65 distinctive landmarks; (b) “Hidden” lesser trochanter in 2D radiograph.

the model to learn the shape variation that is given by the projected proximal femur of this particular person.

2.4 Within-person shape variation

As given in Equation (1), statistical shape models allow to define every shape by the mean shape over the image set as well as a linear combination of shape vector modes, where a specific shape is characterised by shape parameters \mathbf{b} . Since there may be patient positioning differences between two short-term radiographic sessions, we assume that every shape parameter vector \mathbf{b} not only reflects the true shape but also includes some error due to patient positioning variation. Accordingly, every shape parameter vector \mathbf{b} , can be represented as

$$\mathbf{b} = \mathbf{b}_t + \mathbf{b}_e \quad (2)$$

where \mathbf{b}_t characterises the true shape, and \mathbf{b}_e accounts for repositioning errors. For simplicity, we assume that \mathbf{b}_t and \mathbf{b}_e are independent. In this case, the covariances of each term are related as

$$\mathbf{S} = \mathbf{S}_t + \mathbf{S}_e \quad (3)$$

where \mathbf{S} is the covariance of all the data, and \mathbf{S}_e is the within-person covariance due to repositioning. We estimate the latter from the shape parameters for the 21 pairs of images in the usual way (i.e. as the pooled covariance of the difference from the mean for each individual). This allows us to use Equation (3) to estimate \mathbf{S}_t .

The eigenvectors of \mathbf{S}_e define a shape model which can be used to visualise the variation in projected shape due to positioning (see results below). Analogously, the eigenvectors of \mathbf{S}_t define a model of *true* shape variation of the projected proximal femur in a population.

3 Results

Figure 2(a) illustrates the standard deviation (SD) of the shape model modes of the overall model compared to the model modes of the WPV model. This shows that the WPV makes a rather small contribution to the overall shape variation given by the model over 87 radiographs. Figures 2(b)-(d) demonstrate the parameter values for the first six modes of the overall shape model together with the predicted WPV distribution (within two SD of the mean) for every individual of the 21 paired radiographs. At this, Figure 2(c) gives an example of shape modes where the proportion of WPV is quite high compared to the overall variance of these modes. Figure 3 shows the three most significant modes of the WPV subspace, and Figure 4 gives the four most significant modes of projected proximal femur shape variation after allowing for WPV.

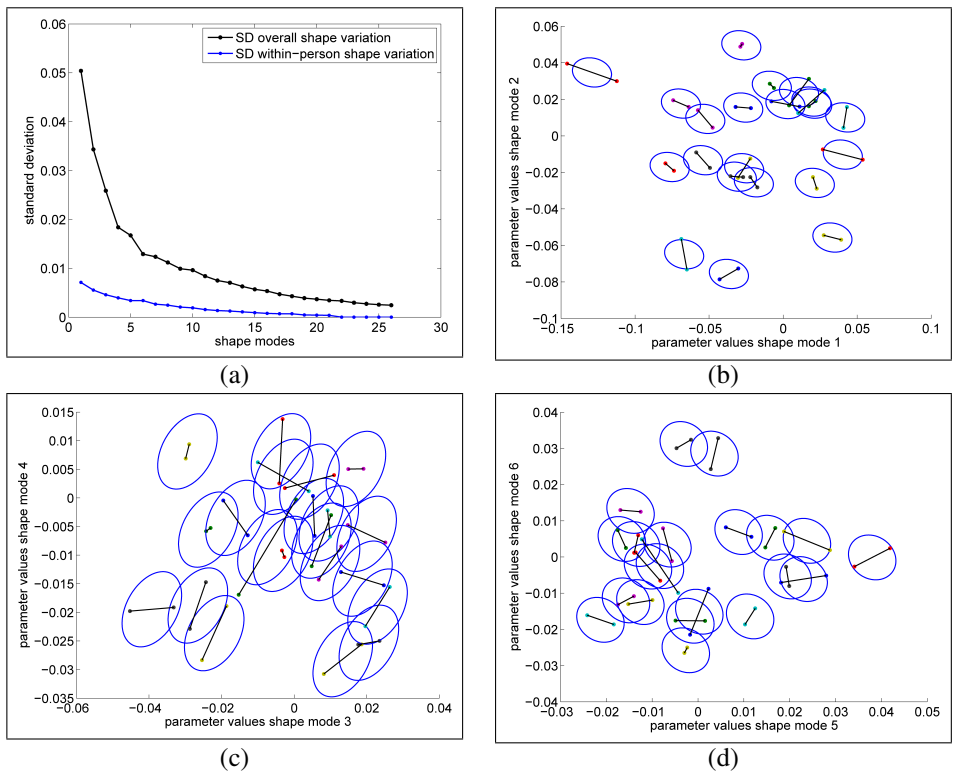


Figure 2: (a) Standard deviation of the overall shape model modes compared to the standard deviation of the within-person shape variation; Parameter values and within-person variation distribution (2 SD) of the overall shape model for all 21 pairs for selected model modes: (b) mode 1 versus 2; (c) mode 3 versus 4; (d) mode 5 versus 6.

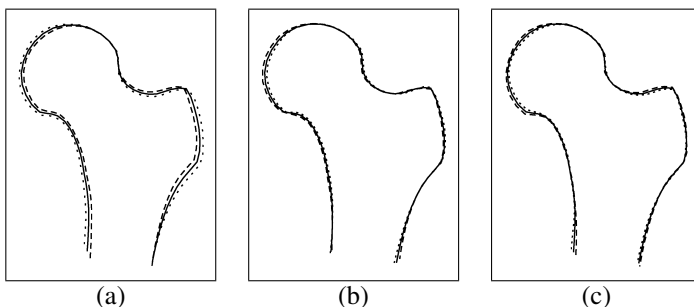


Figure 3: The three most significant modes of the within-person shape variation subspace ((a) most – (c) less significant). Each figure shows the average (—) and ± 6 SD.

4 Discussion

As demonstrated in Figure 2(a), the variation in projected proximal femur shape for an individual is small compared to the overall variation in a population. As can be seen in Figure 3(a), the first WPV mode appears to represent projected proximal femur shape variation due to patient positioning. In contrast, the less significant modes, as for example given

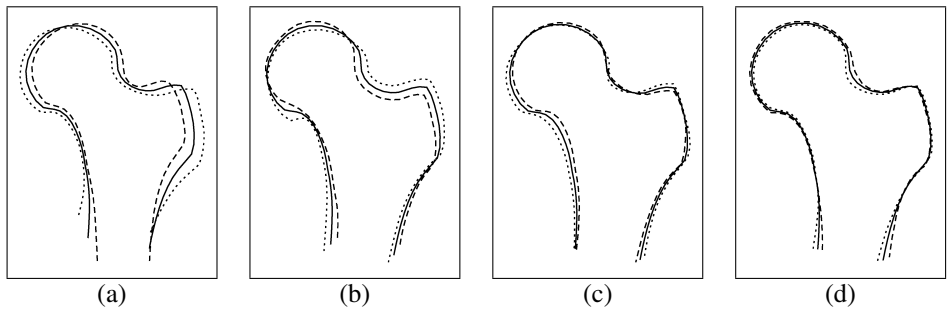


Figure 4: The four most significant modes of the individual proximal femur shape variation subspace ((a) most – (d) less significant). Each figure shows the average (—) and ± 2.5 SD.

in Figures 3(b) and 3(c), seem to be related to annotation errors introduced by the required manual adjustment after the application of an ASM to the second of each image in a pair. Annotation errors may be caused by missing key landmark points (e.g. along the hemispheric shape of the femoral head) or by the absence of a locally distinctive boundary (e.g. along the superior border of the greater trochanter). This work suggests that proximal femur shape in AP pelvic radiographs provides reliable data for the analysis of the relationship between proximal femur shape and hip joint diseases such as osteoarthritis or osteoporosis.

In terms of future work, we hope to extend this study by also allowing for the possibility of individual proximal femur shape variation and WPV to be dependent on each other. Moreover, this work could be extended by setting up an additional shape model for both the lesser and the greater trochanter and by analysing the WPV accordingly.

Acknowledgements

The arcOGEN Consortium is funded by Arthritis Research UK and C. Lindner by the Medical Research Council.

References

- [1] T. Cootes, A. Hill, C. Taylor, and L. Haslam. The use of active shape models for locating structures in medical images. *Image and Vision Computing*, 12(6):355–366, 1994.
- [2] T. Cootes, C. Taylor, D. Cooper, and J. Graham. Active Shape Models—Their training and application. *Computer Vision and Image Understanding*, 61(1):38–59, 1995.
- [3] J. Gregory, D. Testi, A. Stewart, P. Undrill, D. Reid, and R. Aspden. A method for assessment of the shape of the proximal femur and its relationship to osteoporotic hip fracture. *Osteoporosis International*, 15(1):5–11, 2004.
- [4] J. Gregory, J. Waarsing, J. Day, H. Pols, M. Reijman, H. Weinans, and R. Aspden. Early identification of radiographic osteoarthritis of the hip using an active shape model to quantify changes in bone morphometric features. *Arthritis and Rheumatism*, 56(11):3634–3643, 2007.
- [5] J. Lynch, N. Parimi, R. Chaganti, M. Nevitt, and N. Lane. The association of proximal femoral shape and incident radiographic hip OA in elderly women. *Osteoarthritis and Cartilage*, 17:1313–1318, 2009.
- [6] M. Roberts, T. Cootes, E. Pacheco, and J. Adams. Quantitative Vertebral Fracture Detection on DXA Images Using Shape and Appearance Models. *Academic Radiology*, 14:1166–1178, 2007.
- [7] L. Waarsing, R. Rozendaal, J. Verhaar, S. Bierma-Zeinstra, and H. Weinans. A statistical model of shape and density of the proximal femur in relation to radiological and clinical OA of the hip. *Osteoarthritis and Cartilage*, 18(6):787–794, 2010.